CHAPTER 1

INTRODUCTION AND LITERATURE REVIEW

1.1 Surface engineering

Surface engineering refers to the alterations made to the surface of engineering components with the intention to achieve improvement in properties such as high hardness, wear resistance, high-temperature resistance and corrosion resistance, without making any significant changes to bulk characteristics of the structures.

1.2 Various surface engineering techniques

Commonly practiced surface engineering techniques are carburizing, nitriding, flame/induction hardening, physical vapour deposition (PVD), chemical vapour deposition (CVD), galvanizing, diffusion coating, plasma spraying etc. However, these techniques suffer from several limitations, e.g., high processing time, high input energy, high material consumption, poor precision, lack of flexibility, lack in scope for automation and requirement of complex heat treatment cycles. Further, the respective thermodynamic and kinetic constraints of restricted solid solubility limit and slow solid state diffusivity impose additional limitations for these processes (Dutta Majumdar, 2003). In contrast, the surface engineering techniques based on applications of laser beam are free from many of these limitations.

1.3 Laser assisted surface engineering

A laser beam with a high energy density is capable of intensely heating and melting most of the refractory metals and ceramics and deposits them on metallic substrates to produce coatings, which possess high hardness and excellent wear and corrosion resistance. The unique feature of laser beam leads to localized melting and solidification within a shallow depth and hence makes it possible to modify the surface layer without affecting the bulk of the as-received sample (Singh and Dahotre, 2004).

1.3.1 Advantages of laser assisted surface engineering

Laser assisted surface engineering offers several advantages over other surface modification techniques. It is a fast process and can be applied readily on many engineering surfaces without the requirement of elaborate support systems (like ultra-high vacuum environment etc). High cooling rates (10^3-10^8 K/s) attainable in laser heating can give rise to extremely fine grain structures and improved mechanical properties. By employing a high power laser, extremely high temperatures can be attained to melt both the metal substrate and sometimes, added ceramic particles. This may promote chemical reaction and wetting between ceramic and metal, and, as a result, may lead to a strongly bonded ceramic–metal interface after solidification (Agarwal and Dahotre, 1999b). The surface structure can be tailored to the requirements of the application by varying process variables such as laser traverse speed, power, beam size, and precursor composition (Kulka *et al.*, 2003). Another advantage of laser assisted surface engineering comes from the fact that laser beam can be transported to any remote corner through fiber optics.

1.3.2 Classification of laser assisted surface engineering techniques

A wide range of laser assisted surface engineering techniques are available today. Usually, laser surface modification involves utilizing the high power laser beam to heat the surface of a material up to a required temperature, followed by rapid cooling by heat conduction to the bulk. Depending on the maximum temperature attained during thermal cycle, Vilar (1999) classified laser surface modification as shown in Table 1.1

Table 1.1: Laser assisted surface engineering techniques classified according to the power density and interaction time

Process	**Power density (W/mm^2)**	**Interaction time (S)**
Laser transformation hardening	$10 - 10^2$	10^{-2}-1
Laser melting	$10^2 - 10^4$	10^{-3}-1
Laser Alloying	$10^2 - 10^4$	10^{-3}-1
Laser cladding	$10-10^3$	10^{-2}-1
Laser CVD	$1-10^4$	$10^{-1}-10^2$
Laser PVD	10^6-10^7	10^{-8}
Laser shock hardening (peening)	10^7	10^{-8}

However, depending on the procedure of adding coating materials, mode of bonding with substrate material, laser power density, interaction time, type of laser used, laser assisted surface engineering techniques can be classified as follows (Chattopadhyay, 2004):

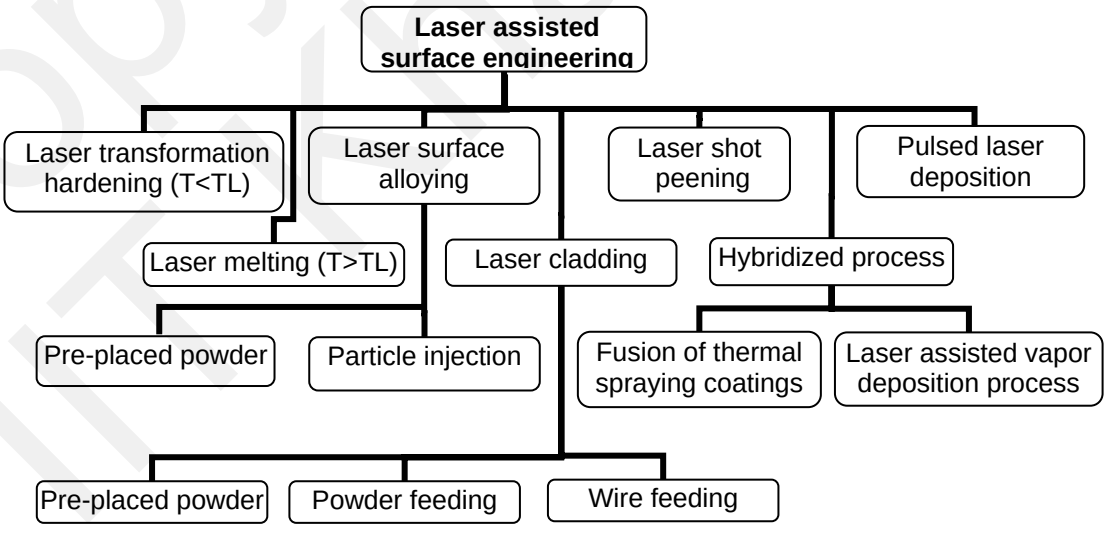

Fig. 1.1: Various type of laser assisted surface engineering technique

1.3.2.1 Laser transformation hardening

Laser transformation hardening is a fairly efficient way of improving the wear resistance of steels. As a result of laser heating and subsequent rapid cooling, a specific austenitic to martensitic structure formation occurs on the surface of the steel. This structure is extremely resistant to seizing, abrasion, and loss of strength in friction (Burakov and Fedosienko, 1983).

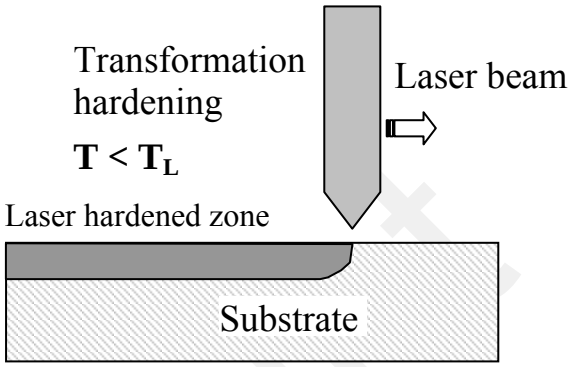

Fig. 1.2: Laser transformation hardening

Laser transformation hardening of steels or cast irons has the same effect as induction or flame hardening, in that the beam heats only the surface layer to form austenite, which then forms hard martensite upon auto-quenching. Fig. 1.2 shows the schematic of laser transformation hardening process where T and T_L represent the temperature rise due to laser irradiation and melting temperature of the material respectively. This technique has found applications where only selected areas of components need to be treated, such as the surface of large piston rings. Sometimes laser surface melting has been applied to grey or spheroidal graphite cast irons, where a thin surface layer is melted and then resolidified at a rapid rate to form hard white cast iron. This has been widely used in the hardening of spheroidal graphite cast iron automotive cam shaft.

1.3.2.2 Laser melting

If a thin surface layer is melted by high intensity moving laser beam, it solidifies rapidly due to mass effect of the bulk material to form non-equilibrium structures. Fig. 1.3 shows the schematic of laser melting process where temperature rise due to laser irradiation (T) should be higher than the melting temperature (T_L) of the

material. Depending on the cooling rate, which largely depends on the laser power, interaction time of laser beam with material, and thermal properties of the material, rapid solidification from liquid state can result in the formation of following three types of metastable metals and alloys.

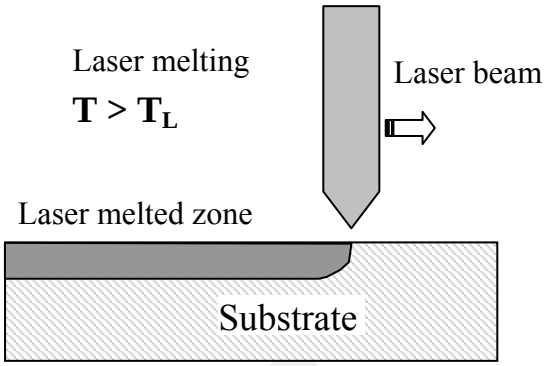

Fig. 1.3: laser melting

Supersaturated solid solutions: If the cooling rate is high enough to prevent nucleation and growth of a second phase, solute atoms are retained in the parent lattice in excess of equilibrium concentration.

Non-equilibrium crystalline phases: Rapid quenching from liquid can lead to the formation of a crystalline phase that does not exist under equilibrium conditions. Surface can be melted and rapidly cooled to produce a non-equilibrium high temperature structure in the melted area.

Amorphous phases: The crystallization process can be suppressed by more rapid quenching from melt, vapor or solution, provided certain kinetic and structural conditions are satisfied. The resulting unstable phases are therefore in amorphous state.

1.3.2.3 Laser surface alloying

Laser surface alloying (LSA) is a laser assisted surface engineering technique that involves melting of a pre-/co-deposited layer of alloying element(s) along with a part of the underlying substrate leading to the formation of an alloyed zone confined to a very low depth from the top surface within a very short interaction time. Laser surface alloying is usually carried out using a continuous wave (CW) laser beam normal to the substrate. When the laser beam scans the surface, it creates a melt pool. Addition

of alloying elements to the melt pool is done either as a pre-deposited layer on the substrate, or by feeding powder into the melt pool. Once irradiation stops, solidification occurs due to rapid heat transfer to the bulk. The solidification front progresses rapidly from the bottom towards the surface, at a very high speed (mainly depending on the scanning speed, depth and shape of the melt pool and material properties). Fig. 1.4 shows the schematic of laser surface alloying with pre-deposited alloying element "B". Here "B" substrate material "A" mixed and forms an alloy of "AB" with improved properties than those of the substrate material.

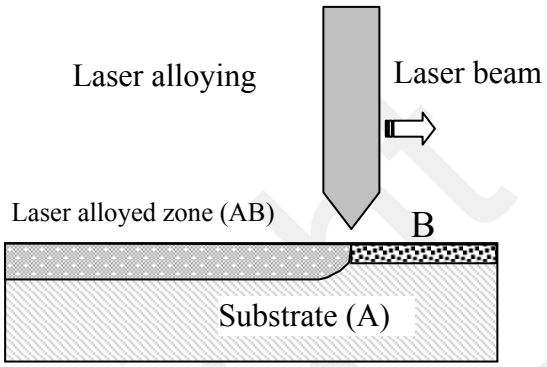

Fig. 1.4: Laser surface alloying

Laser surface alloying is used for increasing the strength of various materials (i.e. - steels, cast iron, titanium, nonferrous metals, alloys, etc.) with a wide range of elements and their compounds because of the relative ease of introducing them into the zone of alloying. Laser surface alloying can be obtained with the aid of laser treatment by two fundamentally different methods:

(i) Introduction of hard particles into the alloying zone

It is imperative to take into account the nature of the interaction between the particles and the molten alloyed material, i.e., the possibility of their dissolution, the formation of chemical compounds, wettability, the difference between coefficients of linear expansion, specific volumes, etc.

(ii) Obtaining the strengthening phases directly in the process of laser alloying

This can be carried out by three methods:

a) Addition of a constituent element of the final strengthening phase to the substrate surface, while other constituent element(s) are contained in the substrate

b) Adding mixtures of the elements

c) Successive additions of the elements.

Here it is necessary to take into account the affinity of elements to each other, and the possibility of the formation of complex chemical compounds.

Moreover, LSA is a non-equilibrium process because it occurs with high heating and cooling rates, and it is also complicated by the formation of the heat affected zone. As a result, compounds with non-stoichiometric composition, metastable and new phases may form in the alloyed zone, i.e., deviations from the phase diagrams are possible.

1.3.2.4 Laser cladding

In laser cladding, laser beam energy is used to locally melt the coating material to form coating of low dilution, with low degree of porosity and crack formation. A thin layer of the substrate must be simultaneously melted to create a fusion bond between the coating and substrate.

The coating material can be supplied by pre-depositing a suitable thickness of the coating material prior to the laser treatment or by depositing an appropriate amount of material (in powder or wire form) directly into the laser beam at its point of incidence on the surface, where it fuses onto the surface to form a clad layer.

There are several advantages of laser cladding as compared to alternative processes such as conventional arc welding or thermal spraying. Thermal input can be precisely controlled by laser cladding, thus yielding minimal dilution and a small heat affected zone. This lower amount of heat input prevents distortion and the base material properties are not detrimentally affected. A clad layer of markedly dissimilar composition to the substrate can be deposited with very little mixing of the two, yet with high bond strength.

Due to the high solidification rates involved, the resulting microstructures are fine and frequently contain non-equilibrium phases and supersaturated solid solutions, leading to high hardness and high wear and corrosion resistance. Depending upon the method of powder application laser cladding can be further classified as:

(i) Laser cladding with pre-placed powder

Laser cladding with pre placed powder (Fig. 1.5) is performed by scanning the laser beam over the substrate surface with a pre-placed layer of precursor powder applied over it. The pre-placed powder is generally mixed with a binder and a volatile non-reactive liquid (like alchohol or acetone) to form a slurry. When the laser beam is incident on the powder surface, melting occurs almost immediately. The melt front advances through the low conductivity powder layer. As the melt front reaches the substrate, heat conduction increases drastically (due to higher conductivity of the substrate material) causing solidification of the melt pool. Good adherence and low dilution are obtained by supplying enough energy to melt a very thin layer of the substrate.

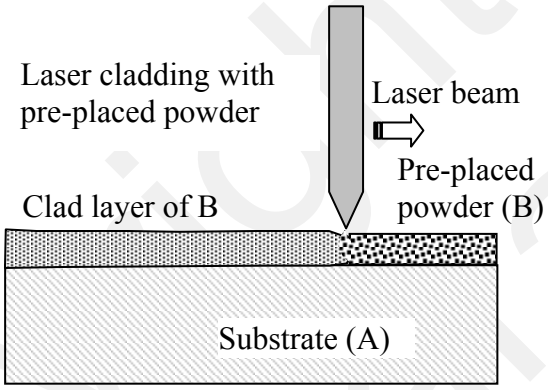

Fig. 1.5: laser cladding with pre-placed powder

(ii) Laser cladding by powder feeding

In this process the clad material is delivered in powder form to the melt pool by means of a carrier gas. The powder jet is directed towards the melt pool surface and impinges on the substrate at an angle (Fig. 1.6). The laser beam scans the substrate in a continuous motion and melts the incoming powder and a thin layer of the substrate to form a clad track. The laser processing parameters are chosen so that the clad material is metallurgically bonded to the substrate, and dilution is sufficiently low to avoid degradation of the clad material properties.

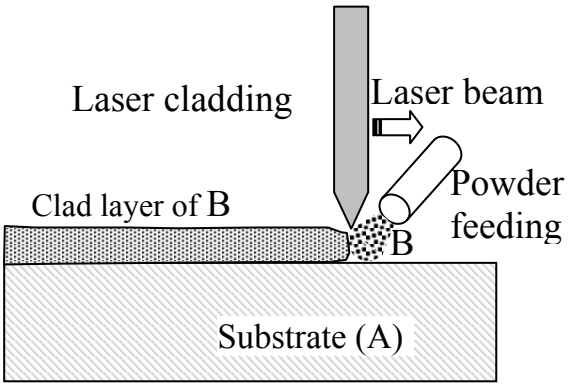

Fig. 1.6: laser cladding by powder feeding

(iii) Laser cladding by wire feeding

In this process, the clad material is supplied to the melt pool as a wire. It is a one-step process and the efficiency of material usage is high, but laser energy is poorly absorbed by wire. To make the process more efficient, the wire and laser beam (with a power density greater than plasma formation threshold) are usually directed at an oblique angle to the surface. A plasma cloud is created in the interaction zone, which couples effectively with the laser beam radiation and transfers its energy to both the wire and substrate. The process is more efficient than the powder interaction technique; however dilution is much higher and extremely accurate alignment of the laser beam with wire is required to get good results.

1.3.2.5 Pulsed laser deposition (PLD)

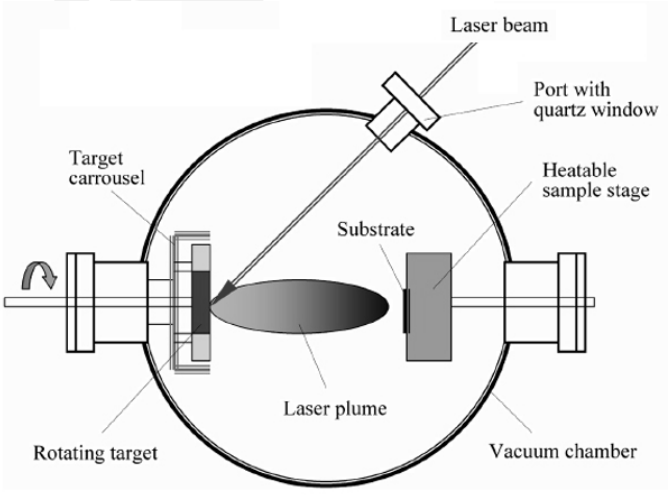

Fig. 1.7: Pulsed laser deposition technique

PLD is a deposition process which uses high power pulsed laser to ablate material from a target to be deposited onto a substrate in a vacuum atmosphere. PLD can be used to deposit a wide range of materials from polymers to metals on substrates at low temperatures. It is a fast process, produces stoichiometrically pure substances with good adhesion but is not good for large area deposition. Fig. 1.7 shows the basic schematic of PLD system.

1.3.2.6 Laser shot peening

Similar to peening by high velocity shots, the laser beam can be used to produce the similar effects on the surface. Laser peening technique involves the generation of tamped plasmas at the component's surface. High laser intensities of 200 J/cm^2 with pulse duration of 30 ns can generate shock pressures up to 10^5 atmospheres when absorbed on a metal surface.

Laser shot peening can induce residual compressive stresses on the surface to a level equivalent to that produced by conventional process i.e., approximately 60% of tensile strength of the material. The process is capable of producing compressive residual stress to a greater depth than that of conventional peening without any significant change in surface finish. Deep residual stress is important for safety of critical items such as compressor and turbine blades. An important additional benefit of laser shot peening is the prevention of crack growth.

1.3.2.7 Laser fusion of thermal sprayed deposits

Metals and alloys deposited by thermal spraying are normally fused by oxy-acetylene flame or induction heating. Ceramic and ceramic based composites with higher fusion temperatures compared to those of metals and alloys are difficult to melt by oxy-fuel flame and these non-conductors cannot be fused by induction heating.

Laser glazing is extensively used for surface fusion and closure of open pores of the thermally sprayed ceramics and related composites. The non-reflective ceramic coatings have the capability of absorbing a large fraction of the laser beam energy. Ceramics being poor conductors, the laser heat gets concentrated at the point of application resulting in melting of the sprayed surface layer. The closing of surface pores prevents ingress of corrosive chemicals & vapors and therefore improves the corrosion resistance of the surface.

1.3.3 Application areas of laser assisted surface engineering techniques

Typical applications of laser assisted surface engineering include:

1. Automotive industry:
    - Hardening and cladding of engine cam shafts and valve seats
    - Hardening of cutting and bending edges on press tools involved in manufacture of automotive parts
    - Surface modification for various tribo-components
2. Aerospace industry:
    - Repairing of turbine blades by laser cladding
    - Hardening of bearing surfaces on rotating shafts
    - Promotion of adhesion between metallic and composite joints
3. Mining, power generation, oil and gas industry:
    - Wear protection of drilling tools or hydraulic cylinders in mining industry
    - Hardening of various parts of pumps, valves and tubular components
    - Hard-facing of steam turbine blades
    - Coating of long drilling tools for oil rigs by laser cladding

1.4 Laser assisted surface engineering for hard and wear resistance coating

A considerable amount of research work has been conducted by various research groups in the field of laser assisted surface modification techniques. With improvements in laser systems in terms of power and beam quality, laser surface modification techniques are now finding increasing applications either in industry to produce hard and wear resistance surfaces for specific applications or as a research tool to develop coatings with novel material combinations on various engineering materials.

With the view to improve hardness and wear resistance of different materials (various type of steel, Al and its alloys, Ti and its alloys), composite coatings of some alloys with unique compositions or ceramic reinforced metal matrix composites have been developed using laser assisted surface modification techniques that include laser surface modification (Rabitsch *et al.*, 1994; Gopalakrishnan *et al.*, 2001; Kulka *et al.*, 2003), laser surface engineering (Agarwal, A., Dahotre 1999a), laser cladding (Xibao

et al., 2001; Manna *et al.*, 2006), laser particle injection (Mehlmann 1990; Ocelik *et al.*, 2005) and laser surface alloying of pre-placed powders (Babu *et al.*, 2006; Roy Choudhury *et al.*, 2007).

1.4.1 Laser coating by laser surface alloying

Laser surface alloying is used for increasing the strength of various materials (steels, cast iron, titanium, nonferrous metals, alloys, etc.). Laser alloying provides an easy way to introduce different phases into the zone of alloying and hence there is a wide choice of elements and compounds that may be introduced into the surface of materials by this method.

Abrasion resistant coatings of Fe-Cr-Mn-C alloy on steel surface (Singh and Mazumdar, 1986) and *in-situ* Fe-Cr-C alloys on AISI 1018 steel (Dahotre and Mukherjee, 1990) have been developed by laser surface alloying (LSA). Due to higher solubility and almost equal melting temperatures of the alloying elements and substrate, homogeneous alloying layers are formed with fine distributions of complex (M6C) carbides in solid solution. In the latter case, chromium powders of different particle size ranges have been used together to obtain optimum packing density of the powder deposited on the substrate. The processing conditions were related to solute (chromium) content, microstructural refinement of the laser alloyed zone and the heat affected zone (HAZ).

Burg *et al.* (1995) have produced a firmly bonded Cr_2O_3 coating on steel (SAF2205) by high power laser processing. A spot size of 1.27 mm diameter with laser power of 1 kW and laser scan speed of 20 mm/s and an overlap of 75% between the tracks have been employed to develop the coating. By measuring the maximum strain energy release rate with a 4 point flexure test, it has been found that the actual interface strength of the laser coating depends strongly on the composition of the substrate and that of the coating material. Delamination occurred by fracture through the coating and partially along the interface, indicating that the interface strength is similar to or higher than the fracture strength of (Fe, Cr)-spinel.

Fishman *et al.* (2001) have developed functionally graded tungsten carbide (WC) alloyed multilayer coatings on M2 high-speed steel by laser alloying with direct injection of WC powder into the melt pool. The laser treatment was performed using a continuous wave CO_2 laser with beam power in the range of 2–7 kW, and a 5 mm

beam diameter. The powder was injected with argon flow as a powder carrier at an angle of 45° through a nozzle (outlet diameter 4 mm) at the distance of 12 mm from the alloyed surface. Powder injection rate of 3 g/min was used in all experiments. Depending on the degree of alloying four different types of structures in laser alloyed coatings were observed. Micro-hardness values in the range of 1100–1200 HV with 40–50% W and 1600 HV with 75% W have been observed. The coating with 58 wt. % tungsten showed a five fold increase in wear resistance as compared with that of the unalloyed laser-melted M2 steel.

TiN-reinforced MMC layer on NiTi has been developed by laser (high-power CW Nd:YAG) coating of pre-placed Ti powder in a nitrogen atmosphere (Man *et al.*, 2006). Commercially available pure Titanium powder of particle size in the range of 40–100 μm was mixed with a binder (4% polyvinyl alcohol) to form slurry and then pasted on the samples. The pasted specimen was dried in an oven at 100 ^{0}C for two hours. The specimens were laser irradiated inside a gas-tight chamber with a glass window through which the Nd:YAG laser beam can pass inside. The chamber was constantly filled up and purged with a mixture of Nitrogen and Argon at a ratio of 2: 1 by controlling the flow rates of Nitrogen and Argon at 20 and 10 l/min, respectively. The ranges of laser power and speed studied were 1–1.5 kW and 20–30 mm/s with a laser spot of 1.5 mm diameter. The laser tracks were overlapped at 50% track width to achieve surfacing. The pre-placed Ti powder reacted with N_2 to form an MMC layer containing a gradient distribution of TiN and $NiTi_2$ dendrites in a Ti rich matrix. The hardness was increased from 250 HV in the substrate to 600–900 HV in the modified layer due to the presence of the hard TiN phase. The large increase in hardness in the coating was mainly due to the presence of TiN, and the change in hardness was consistent with the graded distribution of the hard TiN phase in the matrix. The wear resistance against a diamond ball was correspondingly increased by a factor of two. The higher wear resistance of the MMC layer could be attributed to the complementary effects of the hard TiN phase and the tough metal matrix.

1.4.2 Laser assisted coatings consisting TiB_2, TiC, Al_2O_3 and SiC phases

It is known that coatings based on borides, carbides, and oxides of some refractory materials have high wear resistance. (TiC + steel) composite layer has been formed on the surfaces of Armco iron and AISI 1045 steel by injecting the TiC powder into the

molten surface layer (Ariely *et al.*, 1995) with laser alloying process. Experiments were carried out under a protective atmosphere of argon, which also served as the carrier gas. Laser power of 1.7 kW with a laser-beam diameter 1.2 mm was used for experimentation. Scanning speed of 10 mm/s, powder feed rate of 0.043 g/s, and overlap of 50% between consecutive passes was selected as operating conditions after performing some preliminary experimentation. From the analysis of microstructures the authors have found that some of the TiC particles had partially melted during their passage through the laser beam and had re-solidified, forming small and fine dendrites. Phase identification by XRD and TEM revealed the presence of α-Fe, martensite and Fe_3C phases, as well as some amounts of stochiometric TiC and unknown phases. A correlation was found between the substrate composition, microstructures of the coatings and the different phases inside them.

Carbides (SiC and WC) along with elements (Cr and Ni) have been employed as additive elements during laser surface alloying of AISI 4340 steel under different processing speeds (McCay *et al.*, 1999). The sand blasted surfaces of the substrates were coated with a slurry comprised of chromium (44 wt %), nickel (22 wt %), silicon carbide (3 wt %) and tungsten carbide (8 wt %) powder, varnish and mineral spirits. The laser treatment was performed with CW 3 kW Nd:YAG laser at an overlap index of 2.5mm at 2000W laser power and 1000, 1500, 2250 and 3000 mm/min laser scan speeds. The resultant alloyed surface shows improved hardness, wear resistance and corrosion resistance compared to those of the base AISI 4340 steel material. The added chromium and nickel altered the matrix alloy properties, improved the corrosion resistance, while the carbides increased the hardness as well as the wear resistance. The dissociation of the original carbides (SiC and WC) into elemental silicon and tungsten supplemented the stabilization of ferrite and the reduction in hardness. The presence of undissociated carbides and some martensite formation provided substantial increase in the micro-hardness. The carbides sometimes initiated some cracks. However, crack formation was minimized by achieving better homogeneity during processing.

Agarwal and Dahotre, (1999b) have applied laser surface engineering (LSE) to develop a uniform, continuous TiB_2 reinforced Fe composite coating of 200 μm thickness, on AISI 1010 steel. A 2.5 kW CW Nd:YAG laser equipped with a fiber optic beam delivery system was employed for synthesis of laser assisted TiB_2

coatings. Laser beam power of 1.5 kW and varying laser traverse speed (150-200 cm/min) was used. Polygonal and needle shaped boride particles are uniformly distributed in the laser melted zone. The interfacial microstructure consists of cellular dendrites and fine equiaxed dendrites. Metastable phase(s) such as Fe_xB_y and Ti_mB_n are also observed which is a characteristic feature of non-equilibrium synthesis is by laser energy. The coating exhibits knoop hardness up to 1772 (under 300 gm load) and metallurgically sound interface with the substrate. Compared with the same coating developed by pulsed electrode surfacing (PES) process (Agarwal and Dahotre, 1999a,) the authors have found that LSE yields higher hardness and higher interfacial bonding strength compared to those for coatings obtained through the PES technique. However, with LSE process some metastable phases have also been formed, which is a characteristic feature of non-equilibrium synthesis by laser energy.

Babu *et al.* (2006) have investigated laser surface alloying with a mixture of 80 wt.% 431-type stainless steel and 20 wt.% titanium carbide powders on 1020 steel substrate. The laser deposition was made using 2430 W (Nd:YAG laser) laser power and 2.12 mm/s laser scan speed with beam diameter of 5 mm. The powder material to be melted by the laser process was pre-placed (1.5 cm thickness) on the substrate surface. Shielding gas (N_2) was delivered to the laser surface processing region at 30^0 reverse angle from the direction of processing. Microstructural characterization of the alloy indicated that titanium carbide melted and re-precipitated as fine carbides from the liquid melt during cooling which enhances the hardness of the coating. The treated specimens exhibited a micro-hardness of 670 $HV_{0.3.}$ The properties of the alloyed region depended on the microstructure that evolved during melting and cooling, largely depending on laser beam parameters and the amounts of the alloying constituents.

A uniform, continuous and crack-free composite coating of TiC particles embedded in Al alloy–Ti matrix has been deposited on 6061 Al alloy by laser surface engineering using Nd-YAG laser beam (Katipelli *et al.*, 2000a). A 2-kW CW Nd:YAG laser equipped with a fiber optic beam delivery system was employed for laser treatment of the sprayed substrates. The lenses within the output-coupling module of fiber optic were configured to provide a beam of 3.5 mm wide line in spatial distribution onto the sample surface. Such configuration provides a rapid processing speed and reduces the overlap between the laser passes. The laser beam power and traverse speed were

maintained constant at 1.8 kW and 120 cm/min, respectively. The coated samples were additionally cooled by mounting them on a water-cooled copper plate during laser processing. The various reactions occurring during laser processing were thermodynamically analyzed and related to the experimental observations. Micro-hardness measurements suggested high hardness in the coating and a strong bonding at the coating substrate interface. The investigators observed higher hardness at the top portion of the coating and found evidence of Si at the top portion of the coating, which apparently segregated there during laser processing. SiC, being less dens (3.1 to 3.2 g/cm^3) in comparison to TiC (4.92 g/cm^3), floats to the top of molten coating during laser processing and remains at the top of the coating after resolidification. An attempt was made to semi-quantitatively determine the interfacial strength by performing some micro-hardness indentations along the interface at various loads (50, 100, 200, 300, 500, and 1000 g). Initiation or formation of any cracks or delaminations at the site of indentations was not observed. Wear resistance of the coated surface was found to be high when compared to that of substrate. The coefficient of friction was found to be 0.64. In order to study the interfacial strength of the coating, four-point bend test was carried out (Katipelli *et al.*, 2000b). Strain energy release rate and the stress intensity factor, were computed for this particular coating-substrate system. From the results, the authors found that some cracks, which propagated from the surface, caused delamination of the coating from the surface.

Kadolkar and Dahotre (2002) have deposited TiC coating on aluminium 2024 and 6061 alloy using Nd-YAG laser beam. The effects of laser processing parameters, such as power intensity and speed on the thickness, microstructure and morphology of both the coating and the heat affected zone have been evaluated using a SEM. The authors have used a 2 kW Nd:YAG laser beam with energy density in the range 1714 - 3429 J/cm^2 by changing the laser scanning speeds (100, 125, 150, 175 and 200 cm/min). From the experimental results they have shown that by controlling the process parameters it is possible to produce varied microstructures according to the requirement of the application. In case of 2024 Al alloy substrate, increase in laser scan speed resulted in refinement of dendrites, attributed to the higher cooling rates. Performance of these coatings depend on the particle size, shape and distribution of the reinforcing phase as well as the processing parameters such as laser power, laser scan speed and energy density due to laser interaction (Kadolkar and Dahotre, 2003).

SiC and Al was laser alloyed on nickel-based high-temperature alloy Inconel-625 (Jasim *et al.*, 1993). A 2 kW continuous wave CO_2 laser was used at 2 and 1.7 kW laser power with a beam diameter of 5 mm, and traverse speeds of 1-22 mm/s. Powder mixtures of aluminium with 10, 30 and 50 wt % SiC were used to produce single tracks with powder feed rates in the range 2-8 g/min. Aluminium was studied as a component for the functionally gradient region for its capability to form aluminide with the nickel present in Inconel-625. SiC was chosen as the ceramic for its potential for improving wear resistance when present in substantial volume fractions in particulate form. Laser processing conditions, particularly powder feed rate and interaction time have been studied in order to achieve proper control of the compositional gradient involving dilution of the successive tracks and the dissolution of the ceramic particles in the matrix. Depending on the processing conditions a number of complex microstructural features can appear, involving various phases (e.g. silicon and intermediate phases such as $A1_4C_3$.

Dutta Majumdar *et al*. (2006a) investigated the improvement in the hardness and wear resistance of aluminum alloy by laser surface alloying that produces a MMC layer on the top of the surfaces of the substrates. SiC and a mixture of Al + SiC (at a ratio of 1:1) were pre-deposited (200 μm) on the substrate by dispersing the powders (particle size 25–50 μm) in alcohol with an organic binder and subsequently, applying the coating on the surface using a brush. Laser composite surfacing was carried out by irradiating the pre-deposited Al substrate using a continuous wave (CW) CO_2 laser with laser power of 3 kW, a beam diameter of 3.5 mm, scan speed of 300-500 mm/min and Ar as the shrouding gas. The microstructure of the composite layer consists of a dispersion of partially melted SiC particles in a grain refined Al matrix. SiC particles are partly dissociated into silicon and carbon leading to formation of a low volume fraction Al_4C_3 phase and free Si, redistributed in the Al matrix. The volume fraction of SiC is maximum at the surface and decreases with depth. The micro-hardness of the surface was improved by two to three times as compared to that of the as-received Al. The presence of hard particles in the matrix is responsible for improvement in the average micro-hardness of the coating. A significant improvement in wear resistance in the composite surfaced Al is observed as compared to the as-received Al, which is attributed to improvement in hardness due to grain refinement.

1.4.3 *In-situ* formation of composite coating consisting TiB_2, TiC, Al_2O_3 and SiC phases by laser coating process

Park *et al.* (2000) have made an attempt to produce *in-situ* TiC particulate composite layer by laser irradiating over a thermally sprayed titanium coating on cast iron. The effect of the laser scan speed on the solidification microstructure of the base metal and titanium alloyed beads was examined. The precipitation morphology of TiC particulates generated by the reaction with carbon contained in the cast iron matrix was observed. From the results, it was revealed that composite TiC particulate has been formed on the surface layer by direct reaction between carbon existing in the cast iron matrix and thermally sprayed titanium coating by remelting and alloying using laser irradiation. The microstructure of the alloyed layer consisted of three zones; the TiC particulate precipitate zone (HV 400–500), the mixed zone of TiC particulate C ledeburite (HV 650–900) and the ledeburite zone (HV 500–700). TiC particulates were precipitated as a typical dendritic morphology. The secondary TiC dendrite arms were grown to a polygonized shape and were necking. After that separated arms became cubic crystal of TiC at the slowly solidifying zone. However, in the rapidly solidified zone near the fusion boundary, the fine granular TiC particulates were grouped like grapes.

Xibao *et al.* (2001) have developed Fe-Ti-B composite coating with TiB_2 as whiskers on austenitic stainless steel by laser cladding with a powder mixture of B_4C and Fe-Ti alloy. Both the hardness (maximum cross sectional micro-hardness of 1300 $HV_{0.1}$) and cracking resistance of the Fe-B laser clad coating could be improved by the formation of TiB_2 whiskers. The experimental work shows that the needle-like TiB_2 whiskers could be synthesized in situ using the laser cladding method in the composite Fe-Ti-B coating. The size, shape and volume fractions of TiB_2 whiskers in the composite coating are greatly dependent upon contents of powder compositions, the ratio of B and Ti elements and the laser energy density used. The average ratio of width to length for the synthesized TiB_2 whiskers increases with increasing laser energy density and ratio of B and Ti in this coating.

Singh and Dahotre (2004) have synthesized a mixed carbide coating on plain carbon steel with the Fe-Ti-Cr-C quaternary system employing laser surface engineering (LSE). A mixture of commercially available Fe (55 wt %), Ti (20 wt %), Cr (20 wt %) and C (5 wt %) powders, blended together and suspended in a water-soluble organic

binder was used as precursor. The slurry of precursor material was deposited by air spray on the substrate for uniform green thickness and then dried at 75 ^{0}C for 30 min. A 2.5 kW CW Nd:YAG laser equipped with a fiber optic beam delivery system was employed with scan speed of 1500 mm/min and varying laser power (900-2100 W) for laser surface engineering. *In-situ* formation of Ti and Cr based carbides using LSE produces a coating with high hardness (five times that of the substrate material) and wear resistance. From the analysis of the results it has been found that, the hardness and wear resistance of the samples without chromium carbides were inferior to those of the samples with both TiC and chromium carbides. A substitutional solid solution of chromium in iron (Fe-Cr) was found in all the samples and the relative estimated amount of the phase was higher for the samples without chromium carbides. Metastable phase (characteristic of non-equilibrium synthesis) like martensite was present in the coating and the transition zone.

Liu and Zhang (2005) have synthesized *in-situ* TiB_2/Ni multiphase metal-ceramic composite coating on medium carbon steel surface by laser cladding. Laser irradiation power 1.2–2 kW, laser spot diameter 3–4 mm, lens with focal length of 300 mm and scanning speed 1–2 mm/s were employed for laser treatment. Results of microstructural studies on the coating show that the composite coating is mainly composed of γ-(Ni, Fe) and (Fe, C) solid solution, dendrites and eutectic structures of TiB_2/ γ -(Ni, Fe) or TiB_2/(Fe, C) distributed in inter-granular spacing. The effect of changes in chemical composition on the amount of ceramic, synthesized *in-situ* has been discussed. Hardness of the coating increases prominently (790- 1100 HV) compared with that of the substrate (200-300 HV). This is the mutual result of solid solution hardening in the dendrites and solid solution hardening and dispersion hardening of the second phase in intergranular.

A composite layer of dispersed TiB_2 particles in AISI 304 stainless steel matrix has been deposited on AISI 304 stainless steel by laser surface modification from a pre-placed mixture of K_2TiF_6 and KBF_6 (in the weight ratio of 2:1) using Ar as shrouding environment (Dutta Majumdar *et al.*, 2007). Analysis of the micro-structure of worn out debris confirmed that, the mechanism of wear is predominantly abrasion and subsequently, three body abrasion in laser composite surfaced stainless steel. The authors (Dutta Majumdar *et al.*, 2006b) have also produced a composite layer of uniformly dispersed TiB_2 and TiB particles in Al matrix by laser composite surfacing

on pure Al substrate using same precursor through an external feeder. The micro-hardness and wear resistance of the surface was improved as compared to that of as-received Al substrate.

Selvan *et al*. (1999) have investigated the formation of titanium boride (TiB_2) and titanium nitride (TiN) coating on Ti–6Al–4V by laser alloying of pre-placed BN powder. The alloying was conducted using CW CO_2 laser with different power levels 1.5, 2.0, and 2.5 kW, keeping beam diameter (1 mm) and scan speed (0.5 m/min) constant. To protect the alloy surface from oxidation during processing, argon gas shield at a pressure of 1.5 kg /cm^2 was fed through a coaxial nozzle. The formation of TiB_2 and TiN, investigated using energy dispersive X-ray diffraction (EDX) results were related to the micro-hardness and microstructure. The surface hardness (1500–1700 HV) observed at the boronised layer was five to six times higher than that of untreated Ti–6Al–4V alloy.

Tian *et al.* (2005, 2006) have produced composite coatings of titanium carbide and titanium boride by laser surface alloying of Ti and B_4C powder mixture on pure titanium substrate or with mixture of Ti–6Al–4V with powder mixture of graphite and boron on Ti–6Al–4V substrate. For the first case (Tian *et al.,* 2005), a continuous wave CO_2 laser, with beam diameter of 4 mm, laser power of 1200 W and varying scan speeds (0.85, 3.85 and 6.8 mm/s) with 40% track overlap was employed to melt the surfaces of the samples. During the process of laser surface melting, the pre-placed B_4C was decomposed and dissolved into the melted pool, leading to alloying of the surface of pure titanium with boron and carbon. Argon gas shield at a pressure of 3.0 kg/cm^2 was fed through a coaxial nozzle with the laser beam. For the second case (Tian *et al.,* 2006) scan speeds of 2 and 4.5 mm/s were employed, keeping other parameters unchanged. For both cases the coatings exhibited higher hardness (1600–1700 $HV_{0.1}$ on Ti-6Al-4V) and higher wear resistance compared to those of the substrate materials. Laser scanning speed and the content of alloying elements have an effect on both the microstructure and the wear resistance of the coatings. With the increase in laser scanning speeds, formation of fine microstructure was observed in the coating.

In order to improve the wear resistance of an aluminum alloy, particulate-reinforced MMC coating with TiB_2 particles synthesized *in-situ*, was formed on a 2024 aluminum alloy by laser cladding with a powder mixture of Fe-coated boron, Ti and

Al (Xu and Liu, 2006). The nano-hardness and the elastic moduli of the phases of the coating have been examined. With the increase in the content of Ti and Fe-coated boron powder in the mixture from 30% to 70%, the maximum hardness of the coating increases from 265 HV to 908 HV. The dry sliding wear behaviour of the coating was investigated using a pin-on-ring machine. It has been found that the wear characteristics of cladding were completely dependent on the content and morphology of the TiB_2 particulates, intermetallics in the microstructure and the applied load. At the lowest load (8.9 N), with increasing content of TiB_2 particulate and intermetallic, the weight loss of the laser cladding due to wear was reduced. At higher loads (17.8, 26.7, and 35.5 N), the 2024 Al alloy exhibited superior wear resistance to the particle-reinforced metal matrix composite cladding as over a certain applied load, the particle and intermetallic compounds fall off and lose their ability to support the load.

Du *et al*. (2008a) have investigated the synthesis of hard composite coating reinforced with TiB_2-TiC on AISI 1010 steel using laser surface engineering. Micro-hardness of the composite coating has been found three to four times than that of the steel substrate. Microstructural examination revealed micron sized blocky particles and submicron-sized spherical particles in the matrix. Results show that TiB_2 dissociated when the Al content reached 30 wt % or more. The composite coating with the presence of TiB_2 shows acicular TiB_2 particles embedded in the α-Fe matrix. Coatings produced using precursor of high-Al content reveals a refined cellular structure due to the high-cooling rate induced by short pulse duration. The authors (Du *et al.*, 2008b) have also synthesized a wear, oxidation and corrosion resistant composite coating consisting of TiB_2 and iron–aluminide on AISI 1010 steel substrate using mixture of Al and TiB_2 powder as precursor. Compared with the steel substrate, micro-hardness and wear resistance of the coating are improved significantly. Due to the presence of hard reinforcements, such as TiB_2 and iron–aluminide, the laser-coated samples demonstrate considerably higher wear resistance than the steel substrate. The hard reinforcements (TiB_2, Fe_3Al, Al_2O_3) can play the role of hard barrier to interrupt the ploughing and scratching and therefore improve the wear resistance of the coating. Processing parameters as well as the composition of the precursor have been correlated to the phase composition and microstructure of the coating.

Manna *et al.* (2006) attempted to explore the feasibility of developing an amorphous layer of Fe–B–C, Fe–B–Si and Fe–BC–Si–Al–C on AISI 1010 steel by laser surface

cladding, with an objective to improve hardness and wear resistance. LSC was carried out by melting the pre-deposited layer of elemental powder blends with nominal compositions of 94Fe4B2C, 75Fe15B10Si and 78Fe10BC9Si2Al1C (wt %) due to their known ability to form glass in rapid solidification. The beam 2.5 kW continuous wave Nd:YAG laser equipped with a fiber optic delivery facility was optically shaped to provide a focused rectangular irradiation spot with 3.5×0.6 mm^2 area on the sample surface. Excellent wear resistance with a micro-hardness up to 1150 $HV_{0.3}$ was reported, however no amorphous phase has been found.

1.5 Application of high power diode laser (HPDL) for laser surface engineering

Surface treatment may be carried out by the use of laser beam with uniform high power density. The success of the laser surface treatment depends on appropriate combination of power density, speed and most particularly, spatial power density distribution (De Damborenea, 1998).

Diode lasers have been known for many years and have been used mainly in electronic devices and metrology. The progress in development of semi-conductor materials allowed for the introduction of industrial high power diode laser (HPDL). Diode lasers produced nowadays achieve power levels up to 20 kW. Diode lasers are characterized by a rectangular or linear shape of beam focus having multi-mode energy distribution (Dobrzan´ski *et al*., 2004). As surface modification processes involve wide area processing, high power diode lasers with multimode beam profile having uniform intensity distribution with wider spot sizes facilitate large area surface treatment with better control of heat input resulting in high integrity and uniformity of the coatings. In contrast, complex and expensive focusing techniques are required for tailoring the laser spot sizes in case of CO_2 and Nd:YAG lasers to obtain uniform beam intensity distribution profiles (Kennedy *et al.*, 2004). In addition, Laser surface engineering with CO_2 and Nd:YAG lasers is relatively expensive as compared to that with the diode laser due to the relatively lower efficiency of the CO_2 and Nd:YAG laser, and high capital costs (especially for Nd:YAG lasers). HPDL has approximately 70% absorption compared with 10-15% for the CO_2 laser and 65% for the Nd:YAG laser (Li, 2000). Fiber-coupled HPDL in the kilowatt range, with larger rectangular beam profiles are extremely appropriate tools for laser surface engineering (Seifert *et al.*, 2004).

The interfacial phenomenon of wetting is often the primary factor governing whether a coating will adhere and bond to a substrate in practical applications. Lawrence *et al.* (1999a; 1999b) have shown that the wetting characteristics of a selected range of ceramic, metallic and composite materials can be controlled or modified by high-power diode laser surface treatments. The authors found a correlation between the change in the wetting properties of mild steel and the laser wavelength. Ehlers *et al.* (1998) have reported the use of a 2.4 kW HPDL with a linear shaped beam profile for hardening medium carbon steel M1044 producing a constant hardened depth of 1mm and a track width of 20 mm. Kugler *et al*. (1998) demonstrated the use of a 1.5 kW diode laser for transformation hardening of tool steels. The work shows that higher hardness and wider track can be achieved with the HPDL due to better beam absorption as a result of shorter wavelength than that achieved with a 2 kW Nd:YAG laser (Gaussian beam).

Recently, Roy Choudhury *et al*., have utilized HPDL in order to produce nano-structured metal matrix composite (MMC) coatings of TiB_2-TiB (Roy Choudhury *et al.*, 2007) and TiB_2–Fe_2B (Roy Choudhury *et al.*, 2008) on steel substrates by combined laser and sol-gel technologies. The authors uses a 1.5 kW continuous wave diode laser (at 808 and 940 nm wavelengths) operated at 1.2 kW and at scan rates of 0.5, 1.25, 5 and 10 mm/s, with a rectangular beam spot of 2.5 mm×3.5 mm. Dobrzan´ski *et al*. (2004, 2005) investigated the effect of alloying with tungsten carbide on properties of X40CrMoV5-1 steel surface, using a high power diode laser.

1.6 Application of sol-gel and laser technologies for ceramic/ceramic composite coating

Sol–gel processing has been widely employed to synthesize amorphous or crystalline oxide coatings on metallic substrates and it was found to be effective in increasing the corrosion and oxidation resistance (Ezz *et al.*, 2006a). The sol–gel method has also been used for synthesis of amorphous or nano-sized crystalline oxides. The two main chemical reactions involved in sol–gel technology are the hydrolysis of the precursors with the formation of partially hydrolyzed products and their calcinations. The chemical and structural transformations that take place in the system during the sol–gel process are influenced by many factors. These include chemical composition, nature of the precursors, presence and nature of special additives, chemical procedure and heat treatment schedule (Brinker and Scherer 1990). The conventional methods

for sol–gel coating have some limitations in their application. For example, cracks can form due to stresses developing during drying and thermal treatment, caused by shrinkage and thermal expansion mismatches. An alternative method for sol–gel coatings of crystalline silica films on polymer substrates using ultraviolet laser irradiation has been developed recently (Imai *et al.*, 1999).

Ezz *et al.* (2006b) developed composite coatings consisting of nanostructured TiN and titanium oxide by a novel laser/sol–gel synthesis procedure under non-vacuum condition. Titanium isopropoxide (TTIP) was used as the precursor for titania gel preparation. Sub-micron and nanosize crystals of pure TiN have been precipitated at the interface approximately 2–3 μm on the coating side. Micro-hardness of the order of 1800–2000 $HV_{0.1}$ has been achieved. The authors (Ezz *et al.*, 2007b) have developed a novel method for the *in-situ* production of TiN by the reaction of titania sol-gel with a nitrogenous admixture under laser irradiation on EN43 (AISI 1050) mild steel and 316L stainless steel substrates. The authors found a coating hardness of 17-21 GPa. The same research group (Ezz *et al.*, 2007a) also synthesized a coating of SiC with Cr–Fe–C intermetallic compound in ferrite matrix by chemical reaction of silica sol-gel with chromium oxide. Silica sol–gel prepared from a silicon alkoxide compound (TEOS), typically used in sol–gel chemistry, was used as a liquid precursor for chemical reaction with solid present. Very fine SiC particles ≤1 μm and M_7C_3 carbides were synthesized *in-situ* and dispersed in the ferrite matrix by this process. Micro-hardness up to 1100 $HV_{0.1}$ and wear rate of the order of 10^{-15} m^3/N.m has been achieved.

In addition, Roy Choudhury *et al.* (2007) synthesized nano-structured metal matrix composite (MMC) boride coatings by laser melting of a pre-placed mixture of B_4C+ Ti–6Al–4V powders and sol–gel derived nano-particulate $Ti(OH)_4$. Micro-hardness values up to 1450 $HV_{0.1}$ and high wear resistance as compared to that of the substrate material has been achieved. The authors (Roy Choudhury *et al*., 2008) also developed nano-structured metal matrix composite coating of TiB_2-Fe_2B on steel substrate by laser melting of pre-placed powder mixture paste of B_4C+sol–gel derived nano-particulate TiO_2 on AISI 1050 medium carbon steel and AISI 316L stainless steel substrates. Nano-particulate and sub-micron level TiB and TiB_2 are found dispersed throughout the metal matrix. Micro-hardness in the range of 800-2000 $HV_{0.1}$ with a wear resistance up to 5 times than that of substrate material has been achieved.

1.7 Ceramic and ceramic matrix composite coating

From the review of the past research on laser surface modification techniques it has been found that the laser coating process is capable of producing metal matrix composites (MMC) involving dispersion of hard ceramic particles in a relatively soft metal matrix. Due to the presence of the soft metal matrix, the maximum hardness of such laser-treated coatings is generally limited to about 1500-2000 HV. The properties of the laser surface modified region depend mainly on the chemical composition and microstructure resulting from melting and rapid solidification.

1.7.1 Monolithic ceramic coating

Ceramic materials (e.g., oxides, carbides, and borides of refractory metals) due to their exceptional hardness, excellent wear resistance and stability at high temperature, find extensive applications in surface modification or coating technology. Hard ceramic phases like TiB_2, TiC, Al_2O_3, and SiC have received considerable attention for surface modification in the past for their high hardness and wear resistance. Density, melting point, modulus of elasticity, co-efficient of thermal expansion, hardness and fracture toughness values of these ceramics have been summarized in Table 1.2 and Table 1.3.

Table 1.2: Physical properties of Al_2O_3, TiB_2, TiC, SiC, Al_3Ti and Fe

Material	**Density (g/cm^3)**	**Melting point(°C)**	**Modulus of elasticity (GPa)**	**Coefficient of thermal expansion ($°C^{-1}$) (°C)**
Al_2O_3	3.9	2015	345-409	9.08×10^{-6}(0 -1527)
TiB_2	4.5	3225	367	$4.6–8.1 \times 10^{-6}$(25–1500)
TiC	4.93	3067	439	$8.15–9.45 \times 10^{-6}$(25–1500)
SiC	3.22	2730	401-410	5.48×10^{-6}(25–1500)
Al_3Ti	3.35	1350	110-145	
Fe	7.87	1535		12.6×10^{-6}

Table 1.3: Hardness and fracture toughness values of the monolithic, binary and ternary ceramic composite consisting Al_2O_3, TiB_2, TiC and SiC

Material	Hardness (GPa)	Fracture toughness ($MPam^{1/2}$)	Reference
Al_2O_3	16.2	4	Shackelford and Alexander, 2001
TiB_2	32.4	3.5-5.75	
TiC	31.4	3.8	
SiC	27.5	4.6	
Al_2O_3-TiC	20.5	4.9	(Lee *et al.*, 2001)
Al_2O_3-TiB_2	21.3	4-6	(Gu *et al.*, 2008)
Al_2O_3–SiC	23	5.2	(Ko *et al.*, 2004)
SiC–TiC–TiB_2	22	5.7	(Wäsche *et al.*, 1999)
Al_2O_3-TiB_2-SiC	21.4-22	8.42	(Jianxin *et al.*, 2001)
Al_2O_3-SiC-TiC	19-32	9.6	(Smirnov *et al.*, 1998)

A considerable number of research works have been done to form monolithic TiB_2, TiC, Al_2O_3, and SiC coatings on various substrates.

(i) $A1_2O_3$ coating

Alumina ($A1_2O_3$) posses a high potential for many engineering applications such as surface modification for wear- and/or corrosion-resistant components. Due to the unique property combination of high hardness, low weight, high strength, high stiffness and temperature stability along with excellent resistance to wear and corrosion, Al_2O_3 has become one of the most extensively used ceramics. The use of alumina coatings, produced by different processes for various tribological applications, especially in aerospace and automobile industries is steadily on the increase.

Many research groups have studied the wear behaviour of plasma sprayed alumina coatings (Bull *et al.,* 1996; Tao *et al.,* 2010; Mindivan *et al.,* 2009). A number of research groups have reported on the laser cladding of $A1_2O_3$ on AISI 304 stainless

steel substrates (Feng *et al.*, 1996) or on Mg alloy (Gao *et al.,* 2007*).* The developed coatings exhibit high wear resistance and corrosion resistance as compared to that of the substrate or coatings developed by the plasma-spray process. However, brittleness, lack of defect tolerance owing to low fracture toughness, and low resistance to thermal shocks can cause severe problems in case of components under mechanical and/or thermal loads. Microstructural parameters such as grain size, porosity and particularly, the size and density of flaws, affect strength. Strength and toughness of alumina ceramics can be enhanced by various energy-dissipating mechanisms such as phase transformation, micro-cracking, grain bridging, and most importantly, by particle or fiber reinforcement. Particle reinforcement of alumina has been studied by adding, for example, TiB_2 as fine dispersed phase in the Al_2O_3 matrix (Lee and Zum Gahr, 1994).

(ii) TiB_2 coating

TiB_2 is a refractory compound exhibiting a unique combination of many useful properties. TiB_2 is characterized by a high-melting point, low-specific weight, high hardness, high strength to density ratio, excellent abrasive wear resistance and higher thermal and chemical stability up to 1700 ^{0}C (Vallauri *et al.*, 2008; Du *et al.*, 2008a). By virtue of its high hardness, good oxidation resistance and excellent strength at high temperature, TiB_2 is a potential component in many widely used wear and thermal shock resistant coatings. These coatings have potential applications in boiler, tool materials and shoot-proof in the surface of arms (Fang *et al.,* 2008; Wang *et al.*, 2006; Darabara *et al.,* 2006; Xu and Liu, 2006). Hence, many research efforts have been carried out to prepare TiB_2 coatings on various engineering surfaces by different coating processes. These processing methods include high velocity oxy fuel spraying (HVOF), plasma spraying and magnetron sputter deposition.

Wear properties of electrodeposited TiB_2 coatings on Molybdenum, Inconel and Nickel at various sliding speeds against hardened steel as counter body have been reported by Kirk *et al*. (1981). The authors observed that wear of TiB_2 coatings at high speed is not dependent on the type of substrate for either lubricated or unlubricated test conditions. It also appears that TiB_2 coatings (under lubricated conditions) are not as wear resistant as either the steel ball bearing or the Al203 single

crystal. However, under un-lubricated wear conditions TiB_2 coating has higher wear resistance compared to that of Al_2O_3 coating under high speed (~30 m/s).

TiB_2 coatings have been deposited on various materials by ion-beam-assisted deposition (Riviere *et al.*, 1991) and d.c. magnetron sputtering (Berger *et al.*, 2004) processes. These works mainly deal with the investigations on the mechanism of development of TiB_2 film on the substrate material. Riviere *et al.*, (1991) found ion-beam-assisted deposition allows for the modification of the microstructural state of a growing film by controlling the mixing parameters independently of the deposition conditions. Berger *et al.*, (2004) mainly investigated the influence of substrate bias on the growth, morphology, grain size and texture of d.c. magnetron sputtered TiB_2 coatings.

Panich and Sun (2005) investigated the mechanical properties of TiB_2-based nanostructured coatings fabricated by magnetron sputtering. The authors attempted to enhance the hardness and adhesion of the TiB_2-based nanostructured coatings by controlling the deposition parameters. It has been found that by proper control of the biasing period, a TiB_2 coating with high hardness and good adhesion strength can be produced. Super-hard TiB_2 coatings were deposited from stoichiometric TiB_2 target using an unbalanced d. c. magnetron on Silicon, stainless steel, high-speed steel and tungsten carbide substrates (Mikula *et al.*, 2008). Recently Rybakova *et al.* (2009) have studied the corrosion behaviour of molybdenum and steel materials, protected by electrochemically plated TiB_2 Coatings. The chemical resistance of the TiB_2 coatings on Mo cylinder was characterized by immersion tests in molten aluminium alloy (Al_9Si_3Cu and $AlSi_7Mg$) in a furnace at air atmosphere under dynamic and static conditions. The investigators observed that TiB_2 coatings effectively protect Mo surface against corrosion in molten Al alloys media.

Agarwal and Dahotre (2000) have deposited wear resistant TiB_2 coating on AISI 1010 steel using high energy density processes such as pulse electrode surfacing (PES) and laser surface engineering (LSE). The wear resistance of the TiB_2 coating deposited by LSE has been found to be higher than that of the PES deposited TiB_2 coating.

Lotfi *et al.* (2003) investigated Ni(Cr)-TiB_2 coatings deposited by high velocity oxy-fuel (HVOF) spraying of SHS-derived cermet powders. Three cermets are prepared with compositions namely Ni(Cr)–65 wt.% TiB_2, Ni(Cr)–40 wt.% TiB_2 and Ni(Cr)–

40 wt.% TiB_2 with 5 at.% excess boron by SHS reaction. The SHS products were milled and the resulting powders were deposited onto steel substrates by HVOF thermal spraying. Coatings consisted primarily of TiB_2 particles in a nickel-based binder phase. Abrasive wear behaviour was examined with both alumina and silica abradents. All the coatings had similar, low wear rates with silica abrasive whilst with alumina abrasive significantly different wear rates were observed. The investigator reveals that higher content of TiB_2 improves the wear resistance of the coating, though indentation fracture toughness reduces.

(iii) TiC coating

Due to high hardness, high melting point, and resistance to thermal fatigue and erosion TiC coatings have a high potential for application in fusion reactor containment vessels components (Mathur and McKee, 1991) as well as in case of cutting tools.

A number of research groups have reported on the development of TiC coating by various methods on different engineering materials. Raman *et al.* (1985) have produced TiC coatings on steels, prepared by argon plasma-spraying of dry Ti and TiC powders in open air and have described the corrosion characteristics of the coating. Pure TiC coating has been deposited by pulsed laser deposition (Zergioti *et al.*, 1997). The authors mainly investigated the formation mechanism of TiC coating with different processing conditions and have studied the morphology of the films with SEM and EDS analysis and the crystal structure by XRD and TEM analysis. Upadhya (1991) developed TiC coating by plasma-assisted physical vapor deposition technique and investigated the morphology and tribological properties of the coatings.

Lee *et al.* (1981) and Kinkel *et al.* (1994) deposited TiC coating by chemical vapour deposition (CVD) on cemented tungsten carbide and steel respectively. These works mainly deal with the mechanism of development of TiC layer on the respective substrate materials and studies the dependence of the morphology of the coating on the process parameters. The authors found, that grain structure of TiC was much finer when either the deposition temperature or the total pressure was decreased and the carbon concentration in the reactant gas was increased. Recently Guo *et al.* (2006) have produced TiC coatings using electro-thermal explosion directional spraying

(EEDS) process and found that the coatings have compact structure, high micro-hardness and good bonding with substrate.

Katipelli *et al.*, (2000) have deposited hard and refractory TiC on 6061 Al alloy by Laser Surface Engineering. A composite coating with TiC particles embedded in Al alloy–Ti matrix has been obtained. Wear resistance of the coated surface was found to be high compared to the substrate material and the coefficient of friction was found to be 0.64.

(iv) SiC Coating

SiC is a ceramic known for its good oxidation, corrosion and creep resistance along with high hardness and wear resistance properties (Thawari *et al.*, 2003). A number of research groups have reported the synthesis of monolithic SiC coating by various methods on different substrate materials to improve wear and corrosion resistance.

Costa and Camargo (2003) deposited SiC films onto WC cutting tool in order to improve wear resistance from a commercial sintered SiC target by r.f. magnetron sputtering. Silicon carbide films were deposited on AISI 304 stainless steel and carbon steel from a SiC target in a magnetron sputtering system (Ordine *et al.*, 2000). Riviere *et al.* (1996, 1998) have produced SiC coatings on AISI 321 stainless steel by dynamic ion mixing (DIM) and by ion beam sputtering technique. The coatings exhibited improved wear and corrosion resistance.

1.7.2 Multi-component ceramic composite

A considerable amount of research has been carried out so far to develop monolithic or single phase ceramic coatings by different techniques, and some of the coatings exhibit acceptable performances.

However, the uses of single-phase ceramics, even when fully densified, are limited by the variability of their mechanical strength and their poor fracture toughness in high temperature structural or wear applications. Their susceptibility to brittle fracture can lead to unexpected catastrophic failure. Considerable improvements in mechanical properties of single-phase ceramic materials have been achieved by incorporating one or more of other components into the base material to form ceramic-matrix composites (CMC).

In this connection, mention may be made of ceramic-matrix composites (CMCs) or multi-phase ceramic composites that are reported to possess higher fracture toughness along with high hardness and wear resistance, compared to those of single component or monolithic ceramics (Mestral and Thevenot, 1991).

In addition, multi-component ceramic composites containing reinforcing phases in nano-particulate form can also enhance the fracture toughness of the composite (Zhang *et al.*, 2003). This raises the possibility of obtaining a coating of high hardness with high fracture toughness. Hence, the development of multi-component ceramic composite coatings on metal substrates has generated considerable interest in surface science.

Recently, various research groups have successfully produced multi-component ceramic composites like Al_2O_3-TiC (Lee *et al.*, 2001) Al_2O_3-TiB_2 (Jianxin *et al.,* 2005; Gu *et al.,* 2008), TiB_2-TiC (Lee *et al.,* 2002), TiB_2-SiC (Zhang *et al.*, 1995) Al_2O_3–SiC (Ko *et al.,* 2004), TiB_2-SiC-TiC (Zhang *et al.,* 1996), Al_2O_3-SiC-TiC (Smirnov *et al.,* 1998), Al_2O_3-TiB_2-SiC (Jianxin, 2001), etc by conventional hot pressing or by SHS. It has been found from these reported literatures, that the mechanical properties of the ternary composites are superior to those of the binary composites. Table 1.3 exhibits the hardness and fracture toughness values of monolithic ceramic i.e. Al_2O_3, TiB_2, TiC, SiC and their binary and ternary composites. From the table it is clearly seen that fracture toughness values of the ternary composites is higher than those of the monolithic ceramic or binary ceramics.

1.7.2.1 Two-phase ceramic composite

(i) Al_2O_3-TiB_2

Over the years, the Al_2O_3/TiB_2 composite has drawn the attention of research groups due to its high wear resistance. Addition of TiB_2 particles to Al_2O_3 matrix improves fracture toughness, hardness, and strength over monolithic Al_2O_3 and offers advantages with respect to wear and fracture behavior.

A considerable number of publications on the processing techniques and characterizations of this composite are available. Jianxin *et al.* (1996), Meyers *et al.* (2001) and Wang (2009) have reported processing techniques for Al_2O_3-TiB_2 composites using SHS routes. Jianxin *et al.* (1996) have studied the mechanical

properties of TiB_2-Al_2O_3 composite powders with respect to the TiB_2 content and determined the optimum percentage of TiB_2 for the best mechanical performance. Meyers *et al.* (2001) produced Al_2O_3–TiB_2 composite by the SHS reaction using ($3TiO_2+3B_2O_3+10Al$), which was densified by uniaxial loading immediately following completion of reaction. The densification was enabled by the high temperatures produced by the combustion reaction (~2000°C) which rendered the reaction product (~70% porosity) plastic. The microstructure was characterized by columnar TiB_2 grains embedded in equiaxed $A1_2O_3$; the TiB_2 phase tended to agglomerate in clusters. A few of the TiB2 grains exhibited dislocations, while the $A1_2O_3$ was annealed. TiB_2-Al_2O_3 ceramic cutting tools prepared by hot pressing exhibit substantial improvement in dry high-speed machining of hardened steel (Jianxin *et al.*, 2005). It was shown that both the wear rates and the friction coefficient at the tool–chip interface of Al_2O_3-TiB_2 ceramic cutting tools in dry high-speed machining of hardened steel were lower compared with the corresponding values for the same tool in low-speed machining. The authors report the formation of a self-lubricating oxide film on the tool–chip interface, owing to the tribological–chemical reaction by the elevated cutting temperature and attribute the improvement in wear resistance and reduction in friction coefficient to its formation.

(ii) TiB_2-TiC

TiC-TiB_2 ceramic–matrix composites have been produced by SHS combined with pseudo hot isostatic pressing using Ti, B_4C and carbon powder (Xinghong *et al.*, 2002). The microstructure of synthesized products consisted of the clubbed TiB_2 grains and equiaxed or irregular TiC grains. The optimal ratio of Ti:B_4C=3:1 of the reactant powder was determined by experiments. It has been found that the maximum relative density (96.8 %), hardness (93.5 HRA), compression strength (2.68 GPa), bending strength (450 MPa) and Fracture toughness (5.8 $MPa.m^{1/2}$) attained for the TiC–$2TiB_2$ ceramic are higher than those of TiC–TiB_2 and 2TiC–TiB_2 ceramics. Higher clubbing of TiB_2 grains into TiC-TiB_2 ceramics resulted in a drastic increase in the fracture toughness for TiC–$2TiB_2$ synthesized compacts.

In-situ toughened TiB_2–TiC composites have been fabricated using reaction synthesis of B_4C and Ti powders at high temperatures (Wen *et al.*, 2001). The resulting materials possessed extremely high relative densities and microstructural examination

revealed well developed plate-like TiB_2 grains (due to very high reaction temperature), leading to improved mechanical properties. Higher flexural strengths (453–680 MPa) and excellent fracture toughness (8.4–12.2 $MPa.m^{1/2}$) were obtained for these composites.

Vallauri *et al.*, (2008) studied ceramic matrix composites based on TiB_2-TiC. The available data provide evidence that the combination of high wear resistance and relatively high thermal shock and oxidation resistance renders TiC–TiB_2 composites an excellent candidate for cutting tools.

Dense nano-crystalline TiB_2–TiC composites formed by field activation from high-energy ball-milled reactants have been studied (Lee *et al.,* 2002). Elemental powders (Ti, C and B) were milled to produce nanometric powders without product formation or to effect a reaction during milling to produce nanostructured TiB_2 and TiC. The products of these two mechanical activations were reacted/consolidated or only consolidated under the influence of a high current and a uniaxial pressure. Dense (up to 98.6%) nanocomposites were formed which exhibited micro-hardness of 20.6 GPa. The same composite has also been synthesized by reaction sintering and densify the composites (Zhao and Cheng, 1999). Intermediate boride phases were formed and their amount and stability were strongly dependent on the sintering temperature and time. It was found that the chemical reaction between the starting Ti metal and B_4C particles could be complete after sintering at ~1500 ^{0}C for 1 h, producing a TiB_2-TiC ceramic composite. TiC-TiB_2 coatings were deposited on WC-Co cemented carbide tool bits by non-reactive magnetron sputtering using hot-pressed targets with different TiC: TiB_2 molar ratios (Holleck and Lahres, 1991). Hardness values of the TiC-TiB_2 layers found is a function of composition, constitution and heat treatment.

(iii) Al_2O_3-TiC

Budhani *et al.*, (1984) deposited TiC-Al_2O_3 two-phase coatings on stainless steel and molybdenum substrates by high rate physical vapor deposition. The micro-hardness of TiC-Al_2O_3 coatings increases with increasing TiC content. Konyashin (1996) investigated the physico-mechanical and performance properties of $A1_2O_3$-TiC ceramics thin films deposited by an arc-evaporation PVD technique. The processing technique and composite nature of the coating improves fracture toughness, transverse

rupture strength, hardness and wear resistance of the ceramic indexable cutting inserts.

Al_2O_3-TiC ceramic composite were prepared by SHS followed by sintering, using TiO_2, Al and C as raw materials at 3:4:2.7 molar ratio (Lee *et al.,* 2001). The effect varying the amount of carbon source and cooling time on the products were studied. The highest combustion temperature and combustion velocity were obtained for activated carbon, however no significant changes in microstructure and mechanical properties of sintered Al_2O_3-TiC composite were observed. Hot pressing was found to be very effective in hindering the formation of pores and obtaining a dense sintered body at 1650°C. The composite exhibited high hardness (17- 20 GPa) along with high fracture toughness (4.9 $MPa.m^{1/2}$)

(iv) Al_2O_3-SiC

Al_2O_3–SiC composites containing up to 30 wt. % of dispersed SiC particles, have been fabricated via hot-pressing and machined as cutting tools. The Al_2O_3–SiC particulate composites exhibit higher hardness (up to 23.4 GPa) in comparison to that of monolithic Al_2O_3 because of the inhibited grain growth due to addition of SiC and the presence of SiC as hard secondary phase. The fracture toughness (maximum 5.2 $MPa.m^{1/2}$) of the composites remains constant up to 10 wt. % loading of SiC (Ko *et al.*, 2004). The improved performance of the Al_2O_3–SiC composite tools attributes to the transformation of fracture mode from intergranular fracture for Al_2O_3 to intragranular fracture for Al_2O_3–SiC composites.

Al_2O_3-SiC micro/nano composites have been prepared by axial pressing of sub-micron alumina powder (coated with poly-carbosilane) at elevated temperature with subsequent pressure-less sintering in the temperature interval of 1700 to 1850 ^{0}C (Galusek *et al.*, 2007). Warm pressing at 350 ^{0}C and 50 MPa resulted in green bodies with high mechanical strength and higher density than in green bodies prepared by cold isostatic pressing of the same powder at 1000 MPa. Moreover the sintering of warm pressed specimens yielded composites with higher final density with the microstructure composed of micrometer-sized alumina grains with inter- and intragranular SiC precipitates. High hardness (19.4±0.5 GPa) and fracture toughness (4.8±0.1 $MPam^{1/2}$) have been achieved for the composites containing 8 vol. % of SiC.

Bajwa *et al.* (2005) have investigated the mechanical properties of the nano-composite ceramic Al_2O_3–SiC developed by ball milling and subsequent hot pressing. The significant benefits in wear behaviour compared to that of monolithic Al_2O_3 have been demonstrated, particularly for erosive and abrasive conditions. From the experimental results authors found that the worn track on Al_2O_3–SiC nanocomposites exhibit a surface covered in plastic deformation grooves, while for the same conditions the monolith exhibits intergranular fracture. The dry sliding wear behaviour of SiC–Al_2O_3 composites with 5, 10 and 15% SiC has been studied and compared with monolithic alumina.

(v) TiB_2-SiC

Study was made of the reaction between silicon carbide and titanium diboride compounds of high hardness and wear resistance occurring in the quaternary system Ti-B-C-Si (Ordan'yan *et al.*, 1986). Micro-hardness values measured on the alloys varied depending on the particle size, in the range 20-25 GPa. TiB_2-SiC composites have been produced by reaction synthesis from TiH_2-Si-B_4C system (Zhang *et al.*, 1995). The composite exhibited high hardness (16.5 GPa) with high fracture toughness (8.67 $MPam^{1/2}$).

(vi) SiC-TiC

TiC–SiC composites were fabricated by spark plasma sintering (SPS) in vacuum without additives (Luo *et al.*, 2004). Vickers hardness of the SiC–TiC composites reached upto 28 GPa and maximum fracture toughness value of 6.2±0.6 MPa $m^{1/2}$ has been achieved when content of the TiC rose to 30%.

Chen *et al.* (2009) fabricated TiC–SiC composites using TiC and SiC powders as starting materials in the range of 1650–2000 ^{0}C in Ar atmosphere by arc-melting technique. The hardness of the fabricated TiC–SiC composites was 25–27 GPa.

1.7.2.2 Three-phase ceramic composite

Smirnov *et al*. (1998) in their work have shown that the Al_2O_3-SiC-TiC composite exhibits a three-fold increase in wear resistance as compared to that of monolithic alumina. Moreover, significant toughening is imparted by SiC whiskers that

subsequently improve the mechanical performance of the composite. The Al_2O_3–SiC–TiC composite was fabricated by hot pressing 46.1 vol. % Al_2O_3 powder, 30.9 vol.% SiC whiskers and 23.0 vol.% TiC powder. Significant reaction occurred between the Al_2O_3 and SiC during processing. The resultant composite consisted of nearly unreacted TiC particles, Al_2O_3, plus smaller concentrations of SiC, mullite and possibly a mixture of Al–Si–O–C. The composite exhibited at room temperature an elastic modulus of 409.69 GPa, micro-hardness values of 19–32 GPa, indentation fracture toughness of 9.69 MPa.$m^{1/2}$, compressive strength as high as 2.8 GPa and fracture strength in bending of 680–825 MPa.

Jianxin (2001) produced Al_2O_3-TiB_2-SiC_w ceramic composites with different volume fraction of SiC whisker, and investigated their friction and wear behaviour sliding against cemented carbide at temperatures up to 800 ^{0}C in air and nitrogen atmospheres. The experimental results revealed a decrease in the wear rate of Al_2O_3-TiB_2-SiC ceramic composite with increasing SiC whisker content. Hardness and fracture toughness of the composite increases with increasing SiC whisker content. Fracture toughness value up to 8.42 MPa.$m^{1/2}$ has been achieved with 30 volume percent of SiC content in the composite.

Zhang *et al.* (1996) developed a platelet reinforced ceramic composite of TiB-TiC-SiC by reactive hot-pressing, using TiH, Si and B_4C as raw materials. Experimental results show that the growth of TiB_2 platelets was different in different regions of the composite. The platelets grew very well in the TiC-rich regions and imperfectly in the SiC rich regions, with agglomeration of TiB_2 prohibiting the growth of TiB_2 platelets. The EDS results show that there is no reaction between TiB_2 and SiC while reaction between TiC and SiC, forming solid solutions. Fracture toughness value up to 6.90±0.18 MPa.$m^{1/2}$ along with high hardness of the composite has been reported.

TiB_2-AlN-SiC ternary composites have been prepared by reactive hot pressing at 2000 ^{0}C for 60 min in an Ar atmosphere using TiH_2, Si, Al, B_4C, BN and C as raw powders. The distribution of elements Al and Si were found inhomogeneous, which shows that to obtain a homogeneous solid solution of AlN and SiC in the composites by the proposed reaction, temperatures higher than 2000 ^{0}C or time duration longer than 60 min are needed. High fracture toughness values (6.35±0.74 MPa.$m^{1/2}$ and 6.49±0.73 MPa.$m^{1/2}$) have been obtained in samples with equal molar contents of AlN and SiC (Yue *et al.*, 1999).

1.7.2.3 Four-phase ceramic composite

Bulk ceramic composite Al_2O_3-TiB_2-AlN-TiN consisting of 4 hard phases (Changxia *et al.*, 2007) fabricated by hot-pressing liquid phase sintering, during which AlN and TiN phases are produced by chemical reactions taking place among Al, Ti and N_2. The relations of volume content of Al-Ti-B and Al-Ti-C master alloys and mechanical properties of alumina matrix ceramic materials are analyzed. The influences of Al-Ti-B and Al-Ti-C additions were studied by mechanical property evaluations and microstructural observation. The developed composite exhibited hardness up to 20.1 GPa, and high fracture toughness (8.44 $MPa.m^{1/2}$).

Ceramic composite powders of TiC-TiB_2-hBN-SiC have been synthesized *in-situ* by the combination of two different SHS reactions in one step by Mossino *et al.* (2004a). Simultaneous synthesis of TiC–TiB_2 and hBN–SiC composites was achieved without the application of high pressure or high temperature. The process yielded high purity powders with tailored compositions suitable for the fabrication of ceramic and cermet materials characterized by wear resistance and self-lubricant behaviour shown by the presence of hBN intimately dispersed into the hard ceramic matrix. This process allows avoiding the high temperature furnace technologies traditionally employed to produce hBN composites. The addition of silicon carbide which is an important ceramic for high-temperature applications represents a further improvement of the properties of the final composite material developed. Reactants powders B4C, TiO2, Mg, TiC, C and α-Si3N4 were milled with a planetary mill for 2 h in a grinding vessel of agate with ball-to-powder ratio of 1:1. The powders were uniaxially pressed into green compacts showing a relative density of about 60%. The ignition of the reaction was performed through a graphite rod electrically heated under inert atmosphere of argon. The stoichiometry has been tailored in order to obtain 5–7% by weight of hBN in the final powders after the leaching step (for the elimination of undesired MgO phase and residual Mg).

Meng *et al.* (2006) have reported the formation of a Ni-matrix laser clad layer in which three reinforcing phases, namely, TiB_2, CrB and TiC are present. Tjong *et al.* (2003) reported the formation of an aluminium-based composite with TiB_2, $A1_2O_3$ and Al_3Ti multi-component phases. The composite has been prepared through reactive hot pressing of TiO_2, Al and B powders. Brittle Al_3Ti blocks were also

formed in situ when the B/TiO_2 molecular ratio is smaller than 2. The experimental results showed that the composite reinforced with in situ TiB_2 and Al_2O_3 particles exhibits a relatively stable cyclic response at low total strain amplitudes. The presence of Al_3Ti blocks led to a very slight cyclic hardening followed by softening at total strain amplitude of 0.4%. Moreover, the intermetallic Al_3Ti blocks reduced the fatigue life of in situ composites as they promoted microscopic cracking during cyclic deformation.

A variety of Alumina-based ceramic matrix composite cutting tool materials were discussed by Like *et al.* (2007) such as ZrO_2-$A1_2O_3$-carbide with Mn and Ti oxides, $A1_2O_3$-TiC-TiB_2-ZrO_2 and $A1_2O_3$-TiC-Mo-Ti.

1.8 Self-propagating high temperature synthesis (SHS) and laser assisted SHS

Self-propagating high temperature synthesis (SHS) provides an attractive practical alternative to the conventional methods for producing novel materials, such as ceramics, ceramic-composites and intermetallic compounds, since it offers advantages with respect to process economics and process simplicity.

The underlying basis of SHS relies on the ability of highly exothermic reactions to be self-sustaining and, therefore, energetically efficient (Moore and Feng, 1995). It generates sufficient thermal energy to sustain itself in the form of a propagating reaction (combustion) wave through the extent of the powder mixture. The wave travels through the reactants, completely converting them to the final product. The temperature of the combustion wave may be as high as 5000 K and the speed of wave propagation can be around 25 cm/s. This process offers an opportunity to investigate reactions at extremely high thermal gradients (~ 10^5 K/cm) (Subramanyam and Vijayakumar, 1992; Borovinskaya, 1992; Mossino, 2004).

There are a number of reaction parameters which affect SHS reactions, e.g. reactant particle size, stoichiometry, green density, thermal conductivity, ignition temperature, combustion temperature, heating and cooling rates and physical conditions of reactants (Mossino *et al.,* 2004b). Many of these parameters are interdependent and have significant effects on the final product morphology and properties. Particle size of the reactant powder has a strong effect on SHS process. The particle sizes of the reactants influences the degree of completion of the reaction, the temporal sequence

of the reaction, the temperature profile of the combustion zone and the velocity of the combustion wave. The stoichiometry of the reactants is another important process parameter. Generally the deviation from the stoichiometry results in a decrease of the adiabatic temperature, any excess of either reactants or products will normally decrease the exothermicity of the reaction with a consequent reduction of the adiabatic temperature through a reduction in the heat liberated. The compaction or green density of the powders plays an important role in the combustion synthesis reaction. A green compact produced with significantly high or low densities will ignite with difficulty. This effect of green density on the ignition and propagation of the reaction was attributed to the balance between a good particle contact but not too much to lead to excessive heat loss from the reaction zone due to increased thermal conductivity.

There are different techniques used to ignite SHS reactions, for example ignition by means of radiant flux, resistance heating coil, spark, chemical oven and laser radiation etc.

Laser-induced ignition provides a possibility to obtain high heat flux densities (up to 10^{11} $W.m^{-2}$). Different types of lasers have been utilized, for example neodymium-doped glass laser, ruby laser and cesium bromide laser. SHS of many systems such as Ti + B, Ti + 2B, Ti + C, Ti + 2Si, Zr + C, Zr + 2Si, MO + 2Si, Al + Ni, 2Al + Fe_2O_3B + $BaCrO_4$ and 2Cu + 3CuO were studied using laser-induced ignition (Moore and Feng, 1995).

Powders undergoing chemical reactions have been used in laser sintering and cladding. Shishkovski *et al*. (1999) reported the laser sintering of aluminium and nickel-base filler powders, titanium and nickel-base filler powders to obtain intermetallics of the Ni-Ti and Ni-Al systems by SHS reactions between the constituent powders. Tarasova *et al*. (2000) reported the synthesis of the ceramic PZT (Lead zirconate titanate) as a monolithic composite by selective laser sintering (SLS) of the oxides of lead, zirconium and titanium respectively. The laser treatment induced chemical processes leading to the changes in phase content and lattice structure of the material. Laser-assisted or laser-triggered SHS has also been investigated to obtain *in-situ* synthesis and coating of hard composite materials (Slocombe and Li, 2001; Kab, 2002).

1.9 Reactions for present work

Zhang *et al.* (2004), in their paper suggested a series of probable SHS reactions using boron carbide (B_4C) and boron nitride (h-BN) as reactants, to produce ceramic composites containing borides. From this literature a suitable reaction that can produce Al_2O_3, TiB_2 and TiC as final products from the reactants TiO_2, B_4C and Al has been adopted as follows:

$$4Al + 3TiO_2 + B_4C = 2Al_2O_3 + 2TiB_2 + TiC \qquad \text{...Eq(1)}$$

$$\Delta G^{\theta}_{T} = -1291684 + 161.145\text{T} \ \text{(J/mol)}$$

In this respect it may be mentioned, Wang *et al*. (2004), employed this exothermic reaction to develop a metal matrix composite (MMC) of Al_2O_3, TiB_2 and TiC in aluminum matrix by the conventional sintering route.

Al_2O_3-SiC composite powder was prepared by the SHS process, using SiO_2, Al, and C powders as raw materials (Lee *et al.*, 2000). Thermodynamic data calculated by the authors shows the possibility of reaction (2) and (3) at high temperature.

$$SiO_2 + 2C \rightarrow SiC + CO_2 \qquad Eq(2)$$

$$3SiO_2 + 4Al + 3C \rightarrow 2Al_2O_3 + 3SiC \qquad Eq(3)$$

1.10 Wear characteristics of ceramics and laser alloyed/cladded coatings

Though, many researchers have developed laser-assisted wear resistant coatings with some novel material compositions exhibiting promising hardness and microstructural characteristics, very few (Ocelík *et al.*, 2005, Xu and Liu, 2006) have assessed the wear behaviour of the coatings developed by laser surface modification techniques.

There is no generalized rule that can be globally applied to a tribological phenomenon for the prediction of amount of wear. Wear resistance of a material is the ability to resist gradual removal of material caused by mainly following basic mechanisms (Holmberg *et al*., 1994; Erdemir, 1994).

(a) Adhesive wear

Adhesive wear can be described as plastic deformation of very small fragments within the surface layer when two surfaces slide against each other. The asperities found on

the mating surfaces will penetrate the opposing surface and develop a plastic zone around the penetrating asperity. Dependent on the surface roughness and depth of penetration the asperity causes damage on the surface layer or even the underlying bulk material. In initial asperity/asperity contact, fragments of one surface are pulled off and adhere to the other, due to the strong adhesive forces between atoms. It is thereby clear that physical-chemical adhesive interaction between the surfaces plays a role in the initial build-up process but the energy absorbed in plastic deformation and relative movement is the main cause for material transfer and wear.

(b) Abrasive wear

Abrasive wear occurs when a hard rough surface slides across a softer surface. The harder surface asperities are pressed into the softer surface which results in plastic flow of the softer material around the harder one. When the harder surface moves tangentially, plouging and removal of softer material takes place resulting in grooves or scratches on the surface. Depending on the geometry of the harder surface and the degree of penetration, the removal of material can take different forms, such as plouging, wedge formation or cutting. The two modes of abrasive wear are known as two-body and three-body abrasive wear. Two-body wear occurs when the grits, or hard particles, are rigidly mounted or adhere to a surface, when they remove the material from the surface. Three-body wear occurs when the particles are not constrained, and are free to roll and slide down a surface.

(c) Fatigue wear and delaminating wear

Fatigue crack growth results from repeated loading and unloading of a surface, at a stress level lower than its ultimate strength. Fatigue wear is produced when the wear particles are detached by cyclic crack growth of micro-cracks on the surface. These micro-cracks are either superficial cracks or subsurface cracks. Fatigue can initiate large-scale cracking and may result in the liberation of surface material in the form of wear debris. At the points of concentrated contact, the surface creates a stress field beneath the contact zone where the maximum shear stress occurs. In rolling, where the stress field moves repeatedly over the surface, fatigue of the near-surface material takes place. Material voids or dislocation pile-ups may form the nuclei for the first crack to occur. After that the crack will often propagate quite rapidly, unite with other cracks and liberate surface material. This often results in large craters in the surface.

Delamination wear is a kind of fatigue wear that occurs on a more microscopic scale in sliding contacts when surface asperities repeatedly slide over each other. Small cracks are nucleated below the surface. Further loading and deformation causes cracks to extend, propagate and join with neighboring cracks. The cracks tend to propagate parallel to the surface, resulting in the delamination of long and thin wear sheets.

(d) Erosive wear

Erosive wear is caused by the impact of particles of solid or liquid against the surface of an object. The impacting particles gradually remove material from the surface through repeated deformations and cutting actions. It is a widely encountered mechanism in industry. A common example is the erosive wear associated with the movement of slurries through piping and pumping equipment. The rate of erosive wear is dependent upon a number of factors such as shape of the particles, hardness, impact velocity and impingement angle along with the properties of the surface being eroded.

(e) Chemical wear

Chemical wear occurs due to detrimental chemical reactions in the contact, initiated by the influence of the environment in combination with mechanical contact mechanisms. Rubbing, in combination with the chemical reactions in the contact, results in removal of material and wear debris formation. The chemical reactions at the surfaces may render them softer and weaker and thus decrease their resistance to new crack formation and liberation of surface material in the form of wear products. Oxidation wear is the most common chemical wear process. A thin layer of oxides will be formed on metal surfaces. This is an important protective layer because without it both the friction and wear in metal contacts would be extremely high. If this layer is continuously removed by rubbing action and the contact is exposed to a humid environment, the formation of new oxide layers is speeded up and the result is typical oxidation wear. In certain cases wear can be due to chemical instability of the materials.

Most of the ceramics are brittle because of their covalent and ionic bonds. In the presence of a hard particle or at high asperity contact pressure, fracture by radial and lateral cracks can be the dominant wear mechanism (Wang and Hsu, 1996). For polycrystalline solids, inter-granular fracture is a result of grain boundary cracking

(Breznak *et al.*, 1985). Despite the fact that ceramics are considered brittle materials, one of the wear mechanisms reported in the literature is "plastic deformation" (Cutter and McPherson, 1973; Aghan and McPherson, 1973). Other wear mechanisms of ceramic materials which appear in the literature are fatigue-induced wear (Bayer and Sirico, 1970), chemical reaction induced wear (Sugita *et al.*, 1984) and adhesive wear (Mehrotra, 1987).

Wear resistance of brittle ceramics against abrasion is mainly determined by micro-cracking. During unlubricated oscillation and abrasive sliding contact, friction and wear of the ceramics are defined by inter-crystalline micro-fracture, spalling of grains or particles of second phases, grain fragmentation, formation and quasi-plastic deformation of surface layers consisting of densified wear debris, detachment of these surface layers and delamination fracture due to subsurface cracking. Sensitivity of the ceramics to surface pressure can be reduced by steps which abate micro-cracking and spalling of grains or phases embedded in the matrix (Zawrah *et al.*, 2002).

The ceramic particles formed *in-situ* has a uniform dispersion in the matrix. This restricts removal or pulling out of grains in case of abrasive wear interface. In that case, the wear mechanism appears to be mix-up of micro-cutting, ploughing and grain pull-out (Sivaprasad *et al.*, 2008).

Jianxin (2001) has reported the wear behaviour of Al_2O_3-TiB_2-SiC composites up to a temperature of 800 ^{0}C. It was emphasized that oxidative wear was dominaing at higher temperatures. For sliding contact of materials at high operating temperatures, oxidation plays a significant role, causing changes in the overall wear rate. The importance of oxidation during wear was identified by many researchers and the classification of mild and severe wear was proposed based on measurement of contact resistance, wear debris analysis and microscopic examination.

The effect of applied load on the wear rate of the Al-based composites prepared by other routes has been analyzed by many investigators (Xie *et al.*, 2006; Basavarajappa *et al.*, 2006). It has been emphasized that the wear rate increases with the applied load. Natarajan *et al.* (2009) investigated the dry sliding wear behaviour of the Al 6063/TiB_2 composite by using a pin on disc method at different applied loads of 9.8, 19.6 and 29.4 N for various temperatures. The results indicate that the wear rate

decreases with the increase in the weight percentage of TiB_2, while it increases with the increase in the applied load.

Xu *et al.* (2006) have shown that the wear characteristics of cladding are completely dependent on the content and morphology of the TiB_2 particulates and intermetallics in the microstructure and the applied load. At the lowest load (8.9 N) with increasing content of TiB_2 particulate and intermetallic, the wear weight loss of the laser cladding is decreasing. At high applied load (>8.9 N), 2024 Al alloy displayed superior wear resistance to the laser cladding coating, the dominant wear mechanism of cladding coating is delamination and third-body abrasion.

1.11 Modulus of elasticity (*E*) and fracture toughness (K_{IC}) measurement of the coating

The modulus of elasticity (*E*) and fracture toughness (K_{IC}) are the important properties for a coating material as these are strongly related to the mechanical strength of the coating. Residual stress of a composite coating is also dependent on the E value of the coating material. For a composite material, *E* is changed according to its composition as well as the processing techniques employed. Measurement of modulus of elasticity (*E*) is difficult by conventional methods for a "composite coating" of low area and thickness.

The nano-indentation technique is at present widely employed to determine various mechanical properties, such as hardness, modulus of elasticity, scratch resistance, residual stress, based on the analysis of the indentation load-displacement curves resulting from the nano-indentation test (Bhushan, 1999).

Oliver and Pharr (1992) developed a mathematical model to measure nano-hardness and modulus of elasticity by analysis of the indentation load displacement curves resulting from the nano-indentation test.

Most of the previous studies concerning the determination of hardness and modulus of elasticity have been performed on either thin films (Barshilia *et al.*, 2008; Fischer-Cripps *et al.*, 2006; Sjölén *et al.*, 2007; Raju *et al.*, 2008) or on bulk ceramics or ceramic composite materials (Gong *et al.*, 2003; Ichimura and Ando, 2001; Musil *et al.*, 2002).

Very few works have been done (Biswas *et al.*, 2008; Agarwal and Dahotre, 2000b; Xu and Liu, 2006) to measure modulus of elasticity (*E*) and nano-hardness (*H*) for coatings developed by laser coating technology using nano-indentation technique.

Biswas *et al.,* (2008) calculated the hardness and modulus of elasticity from a load–displacement graph using the method proposed by Oliver and Pharr for the TiN coating developed on Ti-6Al-4V alloy through laser surface nitriding. Modulus of elasticity (*E*) and nano-hardness (*H*) have been evaluated using the nano-indentaion technique for the composite boride coatings developed with various laser traverse speeds (Agarwal and Dahotre, 2000b). *E* values have been correlated to the reaction(s) occurring within the coating region for different laser scan speeds. The investigators also found that theoretical elastic modulus values are lower than the computed elastic modulus values, as the latter includes the effect of dissolution of fine TiB_2 particles in the Fe matrix and metastable phase formation.

Xu and Liu (2006) measure the nano-hardness (*H*) and the modulus of elasticity (*E*) of the phases of the TiB_2 particulate-reinforced metal matrix composite coating developed on 2024 aluminum alloy by laser cladding.

Fracture toughness (K_{IC}), a measure of a materials resistance to crack propagation, is a critical parameter for a ceramic or ceramic composite used for coating. The application of the Vickers indentation technique to measure the fracture toughness of brittle materials, particularly glasses and ceramics, has become widespread because it can be used on small sized samples of materials not amenable to other fracture toughness tests.

Lawn and Fuller (1975), Evans and Wilshaw (1976) and Lawn, Evans and Marshall (1980) have developed mathematical models to determine fracture toughness through indentation technique. The models are as follows

$$K_{IC} = 0.0515\left(\frac{P}{c^{3/2}}\right) \qquad c/a \geq\approx 2 \quad \text{[Lawn and Fuller]} \qquad \ldots Eq(4)$$

$$K_{IC} = 0.079\left(\frac{P}{a^{3/2}}\right)\log(4.5a/c) \quad 0.6 \leq c/a \leq 4.5 \quad \text{[Evans and Wilshaw]} \qquad \ldots Eq(5)$$

$$K_{IC} = \alpha\left(\frac{E}{H}\right)^{\frac{1}{2}}\left(\frac{P}{c^{3/2}}\right) \qquad \text{[Lawn, Evans and Marshall]} \qquad \ldots Eq(6)$$

Where P = applied normal load, a = half-indentation diagonal, c = (crack length + half-indentation diagonal) and α depends on geometry of the indenter. *A* Schematic of crack formation by Vickers indentation is shown in Chapter 2

Cantera *et al.* (1998) determined the fracture toughness of composite coating 86WC–10Co–4Cr produced by the Detonation Gun (D-Gun) process and High Velocity Oxy-fuel (HVOF) process. Fracture toughness of composite coatings deposited by HVOF spraying of SHS-derived cermet powders of Ni(Cr)–TiB_2 in different percentage compositions have been measured (Lotfi *et al.*, 2003). Bolelli *et al*. (2006) have measured fracture toughness for thermally sprayed ceramic composite coating of (Al_2O_3, Al_2O_3–13%TiO_2, Cr_2O_3) by indentation method. The indenter was positioned such that the two indent diagonals were parallel and perpendicular to the substrate–coating interface, respectively.

For all of the above cases, indentation load of 1 kgf have been used to produce parallel and transverse crack of the coating substrate interface. For first case (Cantera *et al.*, 1998) both "Evans and Wilshaw" and "Lawn and Fuller" equations have been employed whereas for other cases (Lotfi *et al.*, 2003; Bolelli *et al*., 2006) only "Evans and Wilshaw" equation has been used to calculate fracture toughness values. However, no specific literature has been found that has employed indentation method to measure the fracture toughness of ceramic composite coating developed by laser alloying/cladding.

It has been found that there is no simple relationship between the mechanical response (like wear resistance) of the coating and *H* or *E* alone; however, this response is strongly dependent on the ratio *H*/*E*. Leyland and Matthews (2000) discussed the importance of the elastic modulus *E* and the ratio *H*/*E* in determining the endurance capability of a surface coating, especially its ability to accommodate substrate deflections under load. Recent experiments, however, show that hard nano-composite coatings with the same hardness, according to their chemical composition, can exhibit different values of the effective Young's modulus (*E*) (Musil *et al.*, 2002). This means that there is a possibility of tailoring the mechanical properties of a material for a given application.

1.12 Problem Definition and Objectives

From the review of the past research on laser surface modification techniques it has been found that the laser surface modification technique is capable of producing hard and wear resistance composite coatings involving dispersion of hard ceramic phases in a relatively softer metal matrix. Due to the presence of the soft metal matrix, the maximum hardness of such laser-treated coatings is generally limited to about 1500-1800 HV. The properties of the laser surface modified region depend mainly on the chemical composition and microstructure resulting from melting and rapid solidification.

From the literature it has also been found that ceramic-matrix composites (CMC) or multi-component ceramic composites can enhance the values of fracture toughness of the composites along with high hardness. This raises the possibility of obtaining a coating of high hardness with high fracture toughness. Hence, the feasibility of multi-component ceramic coatings on metal substrates can be a new area of interest in surface engineering.

A composite comprising of the constituents Al_2O_3, TiC and TiB_2 may also combine ceramic properties such as high melting point, high hardness, thermal and chemical stability, wear and corrosion resistance with typical metallic properties such as high electrical and thermal conductivity. This advantageous combination can make these materials promising candidates as constituents of a multi-component protective coating with enhanced resistance against thermal, corrosion and mechanical wear.

Self-propagating high-temperature synthesis (SHS) technique leads to the *in-situ* formation of refractory ceramics from reactants through exothermic reaction. Laser-assisted or laser triggered SHS has also been investigated by some researchers to obtain *in-situ* synthesis and coating of hard composite materials.

From the literature it has also been found that, high power diode laser (HPDL) with its specific advantages; i.e. uniform intensity distribution, high absorption by metallic surfaces, low operating cost and easy to transport through fiber optics proves to be an extremely appropriate tool for laser surface engineering.

Nano-sized precursors, with a high surface-to-volume ratio in the powder mixture, ensure better mixing between the powder constituents. This causes a fast initiation and completion of the SHS chemical reaction. Sol-gel technology is a chemical route

to produce nano-sized TiO_2 and SiO_2, which could be used as precursor powder for laser triggered SHS reaction.

In the case of multi-component ceramic composites, a number of research groups have experimented with the addition of SiC to the matrix of coatings for improvements in the coating properties. It is interesting to note that apart from the increase in hardness, significant toughening can also be imparted by the addition of SiC to a material. Ceramic composite powder consisting of four phases has been synthesized *in-situ* by the combination of two different SHS reactions by some research groups. Bulk ceramic composites consisting of four hard phases may exhibit higher hardness with higher fracture toughness.

Hence, after review of the aforementioned literature and progress in the field of laser assisted surface engineering, it has been decided to develop multi-component ceramic composite coatings with the novel compositions of Al_2O_3-TiB_2-TiC and Al_2O_3-TiB_2-TiC-SiC *in-situ* through SHS reactions and subsequent laser cladding. The SHS reactions considered for the Al_2O_3-TiB_2-TiC composite coating as per Eq(1) and for the Al_2O_3-TiB_2-TiC-SiC composite coating as per combination of both Eq(1) and Eq(2) as suggested by Zhang *et al*. (2004) and Lee *et al*. (2000) .

To the best of the authors' knowledge these combinations of hard phases i.e. Al_2O_3-TiB_2-TiC and Al_2O_3-TiB_2-TiC-SiC in a coating have not been attempted earlier and are going to be investigated in the present work for the first time.

With these motivations, the major objectives of the present investigation are set as follows

1. To investigate the feasibility of the development of *in-situ* Al_2O_3-TiB_2-TiC multi-component ceramic composite coating on mild steel (AISI 1020) substrate, by combined SHS and laser cladding of pre-placed powder mixture.
2. Development of Al_2O_3-TiB_2-TiC composite coating using high power diode laser (HPDL) on AISI 1020 mild steel
3. To study the effects of sliding speed and normal load on the tribological performance of the composite coating developed with different laser process parameters (laser power and laser scanning speed).

4. To measure the modulus of elasticity (E) nano-hardness (H) and fracture toughness (K_{IC}) of the composite coating.
5. To study the effects of variation in size of TiO_2 powder in the precursor powder mixture on the properties and performance of the coating.
6. To study the effects of substrate materials (AISI 1020 and AISI 304) on the formation, properties and performance of coatings.
7. Development of Al_2O_3-TiB_2-TiC-SiC composite by double SHS reactions and to study the effect of additional SiC on the performance of the coating.